2008

A Study of Frost Nucleation on Flat Surfaces: Theoretical Model and Experimental Validation

Robson O. Piucco
Federal University of Santa Catarina

Christian J. L. Hermes
Federal University of Santa Catarina

Claudio Melo
Federal University of Santa Catarina

Jader R. Barbosa
Federal University of Santa Catarina

A Study of Frost Nucleation on Flat Surfaces: Theoretical Model and Experimental Validation

Robson O. PIUCCO*, Christian J. L. HERMES, Cláudio MELO, Jader R. BARBOSA Jr.

POLO Research Laboratories for Emerging Technologies in Cooling and Thermophysics,
Federal University of Santa Catarina, 88040-900, Florianópolis, SC, Brazil
Phone: +55 48 3234 5691, e-mail: hermes@polo.ufsc.br

(*) Whirlpool S.A., Rua Dona Francisca 7200, 89219-901, Joinville, SC, Brazil

ABSTRACT

This paper advances an investigation on the frost nucleation on flat surfaces. The study focuses on the relevant parameters affecting the frost formation process, i.e., the surrounding air temperature and humidity, and the surface conditions (temperature, roughness and contact angle). The process of ice crystal nucleation was investigated both theoretically and experimentally in order to provide a physical basis for a criterion for predicting the occurrence of frost nucleation as a function of the operating conditions and surface characteristics. A mathematical model for the heterogeneous frost nucleation on smooth surfaces was put forward based on the classical nucleation theory. Experiments were carried out using a purpose-built apparatus to acquire data to validate the model. When compared to in-house as well as independent experimental data, the model predictions showed a reasonable level of agreement.

1. INTRODUCTION

Household refrigerators are labeled as frost-free when frost occurs on the evaporator coil only. However, under certain environmental, operating and constructive conditions, frost is sometimes found on the cabinet liners, increasing the field call rates and the maintenance and quality assurance costs. To avoid this inconvenience, manufacturers are being compelled to improve the design of their products and, at the same time, maintain or even reduce the production costs and the energy consumption. The presence of frost is also undesired because it deteriorates the equipment performance (e.g., frost accretion on evaporators of household refrigerators). In any case, it is worthy to delay or, if possible, to avoid the ice crystal nucleation and the subsequent growth and densification of a frost layer on a surface. A better understanding of the frost nucleation process is, therefore, vital for solving a wide range of technological problems.

Fletcher (1970) presented a pioneering study on the frost nucleation on chilled surfaces focusing not only on the physico-chemical structure of ice crystals but also on the theoretical aspects of the water vapor phase change phenomena, i.e., condensation and desublimation. During the following three decades, however, very little was accomplished regarding the elucidation of the frost nucleation mechanisms. Recently, the subject was revisited by Na and Webb (2003), who presented a fundamental description of the frost nucleation process on flat surfaces in terms of several parameters. Also, Na and Webb (2003) modeled the different types of water vapor phase change phenomena (i.e., condensation and freezing, and desublimation) based on specific criteria for each phase transition. The authors classified frost formation as a heterogeneous nucleation process chiefly influenced by the contact angle. In addition, the authors evaluated experimentally the frost nucleation on aluminum sheets covered with different types of coating in order to predict the influence of the contact angle. However, their model overpredicted their own experimental data by as much as 80%.

In a recent mesoscale visualization study, Yu et al. (2007) observed that the transition from water vapor to frost follows five independent stages: droplet condensation, droplet growth with coalescence of supercooled droplets,

droplet freezing, formation of frost crystals in the frozen droplets, and crystal growth with simultaneous collapsing. The authors tested two different surfaces with contact angles of 56 (hydrophilic) and 110° (hydrophobic) under supercooling degrees of up to 40°C. They reported that, in comparison to bare copper (56°), the hydrophobic surface (110°) had a sparser distribution of condensate droplets but larger droplet sizes and smaller droplet heights, which delayed the droplet freezing and frost formation. The authors also presented a theoretical model for the frost nucleation based on the classical nucleation theory, but without a systematic evaluation of its prediction abilities.

In addition to the previous works, some empirical studies on frost formation are available in the open literature. For instance, Lee et al. (2004) investigated experimentally the frost formation on two different surfaces with contact angles of 23 and 88°. The surfaces were submitted to different working conditions (surface temperature and air stream velocity, humidity and temperature), for which different types of frost have been observed. The authors also reported a weak influence of the contact angle on the frost nucleation. It should be mentioned, however, that the working conditions of Lee et al. (2004) were far beyond the theoretical limit of desublimation; a region where the contact angle has no significant effect on the crystal nucleation process.

Liu et al. (2005) applied an acrylic coating on a metallic plate to obtain a hydrophobic surface, which was subsequently tested under different working conditions. Based on their empirical observations, the authors concluded that frost nucleation did not occur when the supersaturation degree is low. In a later study, Liu et al. (2006) spread a thin layer of wax over a bare copper plate, which was also submitted to different working conditions. Similarly to Lee et al. (2004), Liu et al. (2006) did not observe any effect of the contact angle on the frost nucleation process. Again, the working conditions were set beyond the limit of desublimation, which explains their conclusions.

Albeit several important publications concerning frost formation may be found in the open literature, none of them explored the process under the typical working conditions and overall characteristics of household refrigerators and freezers. Additionally, an experimentally-validated criterion for predicting frost nucleation as a function of the psychrometric (air temperature and humidity) and surface conditions (temperature, contact angle and roughness) is yet to be proposed, which is the main focus of the present study.

This work is divided into two parts. Firstly, the process of ice crystal nucleation is investigated theoretically in order to provide the physical basis for a criterion for predicting frost nucleation as a function of the psychrometric and surface conditions. Thus, a mathematical model for calculating the heterogeneous frost nucleation on smooth surfaces was put forward based on the classical nucleation theory (Fletcher, 1970). Secondly, experiments were carried out with five samples with different surface finishings using a purpose-built testing facility. The model was then validated with experimental data obtained in this work and elsewhere (Na and Webb, 2003).

2. FROST FORMATION FUNDAMENTALS

Certain temperature and humidity conditions are required to initiate the frost formation process. In cases where the surface temperature is above the dew-point, only sensible heat transfer occurs. If the surface temperature is below the dew-point, but above 0°C, vapor condensation takes place. On the other hand, if the surface temperature is below 0°C, the condensed vapor may freeze. Finally, in cases where both surface and dew-point temperatures are below 0°C, vapor desublimation may occur, i.e., the water vapor may change straightforwardly into solid. In both cases, there must exist a temperature difference ΔT_{sup} between the surface and the dew-point, the so-called supercooling degree, before the phase change occurs.

As illustrated in Fig. 1, this temperature difference induces a humidity ratio difference $\Delta\omega_{sup}$ between the air stream and the surface, which is called supersaturation degree. Nucleation can be regarded as a result of three independent psychrometric processes. Firstly, the water vapor present in the air stream (A) is cooled down to the dew-point (A'). This process takes place within the thermal boundary layer. As a result of the free surface energy, nucleation is initiated only when an energy barrier is overcome, which depends on an additional cooling down to point (B). When the energy barrier is surpassed, the phase change process takes place (B-C). The overall energy required for the process to occur is a combination of sensible heat (A-B) and latent (B-C) heat parts.

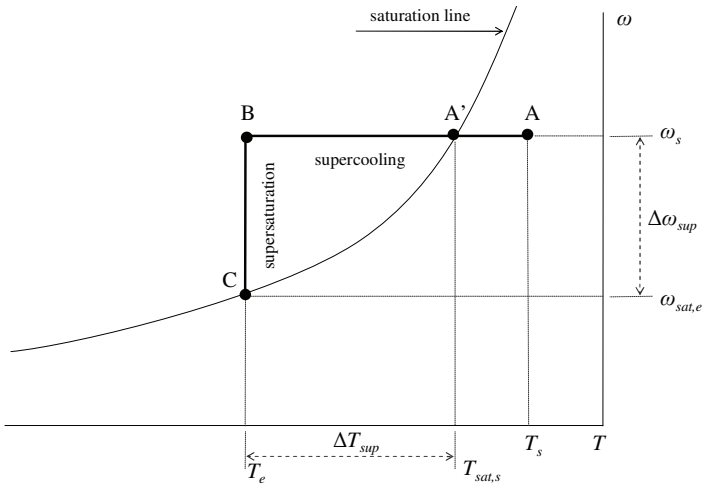

Figure 1. Psychrometic representation of the frost nucleation process

The frost formation process over a flat surface can be divided into the following steps, illustrated in Fig. 2. Firstly, as soon as the necessary non-equilibrium conditions are satisfied, a heterogeneous nucleation takes place (1) and the embryo starts to grow (2). During this process, the embryo surface temperature becomes higher than the plate temperature as its surface increases, demanding a higher amount of energy to maintain its growth. When this amount becomes higher than the energy required to start nucleation on a new site, the embryo stops growing and a secondary nucleation takes place (3). Again, as the new embryo grows (4), so does the energy needed to sustain its growth and, as a result, new nucleation spots appear on the surface of the original embryo (5, 6). The successive nucleation and embryo growth processes go on until the supercooling and the supersaturation degrees approach zero (7). From this point on, the frost layer behaves as a porous medium into which diffusion of water vapor leads to an increase of both thickness and density.

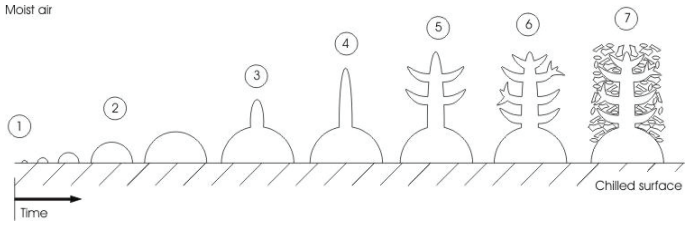

Figure 2. Schematic representation of the frost nucleation and growth processes (Tao et al., 1993)

3. NUCLEATION MODEL

The nucleation of water vapor may follow either a homogeneous (e.g., snowflake) or a heterogeneous process (e.g., frost). In both cases, the energy required to change n molecules from vapor to solid is expressed by the Gibbs free energy, $G=U+PV-TS$, whose differential is given by $dG=VdP-SdT$. Since the phase change process is isothermal, $dG=VdP$, the latent free energy, ΔG_{lat}, can be obtained from

$$\Delta G_{lat} = -\frac{\rho VRT}{M}\ln\left(\frac{\omega_s}{\omega_{sat,e}}\right) \tag{1}$$

where ρ, V and M are respectively the embryo density, volume and mass. R is the universal gas constant, T is the embryo temperature, and ω_s and $\omega_{sat,e}$ are the humidity ratios of the surrounding air and of the air at the embryo surface, respectively.

As depicted in Fig. 3, under thermodynamic equilibrium, the embryo tends to a minimum energy state in which either a spherical or a semi-spherical shape is attained, corresponding to a homogeneous or a heterogeneous nucleation, respectively (Fletcher, 1970). A_{se} represents the interfacial area between the surroundings (s) and the

embryo (e) with a surface energy γ_{se}. A_{ew} and γ_{ew} are the surface area and energy of the embryo-wall interface. γ_{sw} is the surface energy of the surroundings-wall interface.

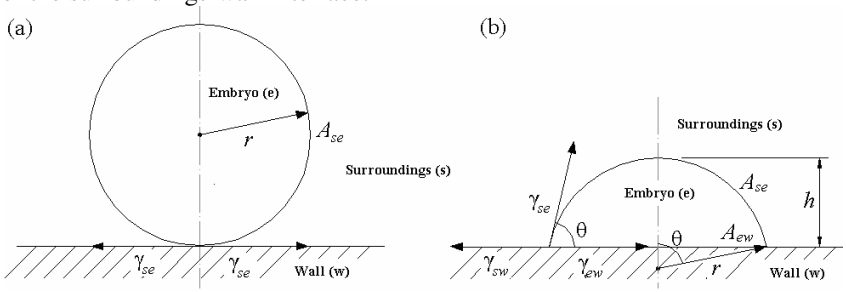

Figure 3. Schematic representation of a homogneous (a) and a heterogeneous (b) nucleation (Fletcher, 1970)

When a heterogeneous nucleation takes place, surface tension effects are present at the three interfaces, resulting in an embryo with both surface area and volume smaller than those observed for a homogeneous nucleation. As a consequence, the energy required to initiate the nucleation process is lower. For a semi-spherical embryo of radius r, the total nucleation energy can be calculated from

$$\Delta G_{tot} = \frac{\rho VRT}{M}\ln\left(\frac{\omega_s}{\omega_{sat,e}}\right) + \gamma_{se}A_{se} - (\gamma_{sw} - \gamma_{ew})A_{ew} \tag{2}$$

where the additional terms, in comparison to equation (1), are due to work associated with the surface tensions at the embryo interfaces (see Fig. 3.b). Noting that the contact angle and the geometrical parameters of the embryo are given by $\theta=\cos^{-1}(\gamma_{sw}-\gamma_{ew})/\gamma_{se}$, $V=\pi h^2(3r-h)/3$, $A_{se}=2\pi rh$, $A_{ew}=\pi r^2 sin^2\theta$, and $h=r(1-\cos\theta)$, it can be shown that the total nucleation energy, ΔG_{tot}, is given by

$$\Delta G_{tot} = \left[-\frac{\pi}{3}r^3\frac{\rho RT}{M}\ln\left(\frac{\omega_s}{\omega_{sat,e}}\right) + \gamma_{se}\pi r^2\right](1-\cos\theta)^2(2+\cos\theta) \tag{3}$$

For certain working conditions, there is a critical embryo size that maximizes the energy required to initiate nucleation. The critical radius, r^*, is obtained making $d(\Delta G_{tot})/dr=0$, which yields

$$r^* = 2\gamma_{se}\left[\frac{\rho RT}{M}\ln\left(\frac{\omega_s}{\omega_{sat,e}}\right)\right]^{-1} \tag{4}$$

The minimum energy required for the onset of nucleation is obtained substituting the above equation into equation (3),

$$\Delta G^*_{tot} = \frac{4\pi}{3}\frac{\gamma_{se}^3}{\left[\frac{\rho RT}{M}\ln\left(\frac{\omega_{sat,e}}{\omega_s}\right)\right]^2}(1-\cos\theta)^2(2+\cos\theta) \tag{5}$$

Equation (5) expresses the minimum energy barrier to be overcome for the onset of nucleation on a smooth surface as a function of the supersaturation degree and contact angle. Figure 4 shows the variation of the term $(1-\cos\theta)^2(2+\cos\theta)$ as a function of θ, where a maximum exists for $\theta=180°$ (homogeneous nucleation).

As observed empirically by Volmer and Flood (1934), there is a minimum rate of embryo formation (2.2 embryo/cm^{2}s) required to initiate a homogeneous nucleation process. For heterogeneous nucleation, however, Becker and Doring (1935) proposed the following exponential relationship for the embryo formation rate,

$$I = I_\circ\, exp\left(-\frac{\Delta G^*_{tot}}{kT_w}\right) \tag{6}$$

where $I_o=10^{25}$ embryo/cm^{2}s is the kinetic constant of desublimation and $k=1.381\ 10^{-23}$J/K is the Boltzmann constant.

Combining the Becker and Doring (1935) equation and the minimum embryo formation rate observed by Volmer and Flood (1934), the limiting energy barrier required to commence nucleation can be expressed in terms of the supercooling degree as a function of the contact angle. Figure 5 shows the nucleation limits as a function of the supercooling degree and of the contact angle. The desublimation and condensation limits were obtained using the densities of ice and water, respectively. It can be seen that unless θ is nil, there must be a certain supercooling degree to start the phase change process.

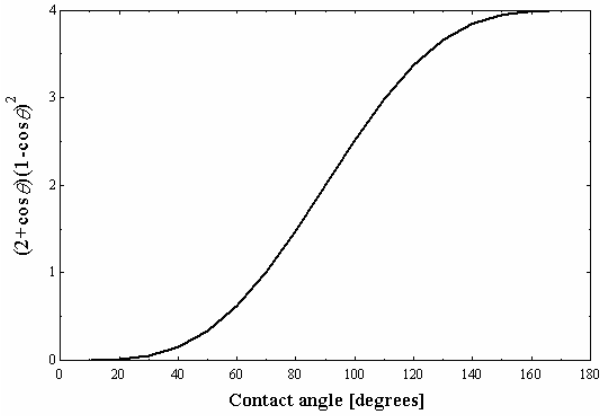

Figure 4. Variation of $(1-\cos\theta)^2(2+\cos\theta)$ with θ

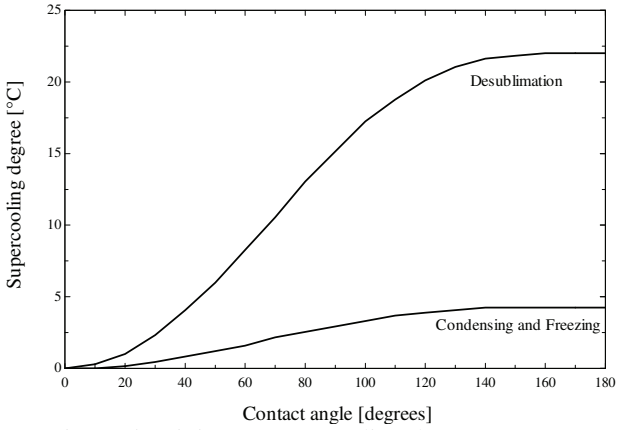

Figure 5. Minimum supercooling degree to start nucleation on a smooth surface as a function of θ

It should be emphasized that equation (5) is applicable to smooth surfaces only. However, most surfaces used in household refrigerator manufacturing have imperfections (i.e., possible nucleation sites) that generally reduce the embryo volume and the surface energy and are, therefore, more prone to frost nucleation. Because of this, an experimental study was carried out to evaluate the effect of surface roughness on nucleation and to verify the applicability of the Volmer and Flood (1934) constant to non-smooth surfaces.

4. EXPERIMENTAL WORK

The test rig was conceived as an open-loop wind tunnel (Fig. 6), which was placed inside an environmental chamber with a rigid control of the operating conditions (air humidity and temperature) upstream of the test section (Fig. 7). The facility was designed to emulate the typical operating conditions of the freezer compartment of a refrigerator, with air velocities between 0.2 and 1.0 m/s, relative humidities between 40 and 90%, air temperatures between -20 and 30°C, and plate surface temperatures between -30 and 0°C. The plate is cooled by a thermoelectric device which is comprised of an aluminum plate on the cold-side, and an air-source heat exchanger on the hot-side. The air flow is driven by an axial fan. The duct was made from stainless steel, and two screens were placed upstream of the test section to homogenize the velocity field. The test section itself was made from Perspex plates to allow the visualization of the frost formation process.

The frost layer deposited on the plate surface was photographed at every minute by an automated data acquisition system comprised by a 4.1 megapixel digital camera equipped with a 32x set of lens and a length scale with a minimum division of 10 μm. The frost thickness measurement was carried out by image processing using the Nikon NIS Elements Basic Research software. A measurement uncertainty of ±5 μm was assigned to the frost thickness. In addition, the temperatures were measured by T-type thermocouples with an uncertainty of ±0.2°C, and the relative humidity was measured by capacitive transducers with an uncertainty of ±1%. A hot-wire anemometer with an uncertainty of ±0.1 m/s was used to measure the air velocity at the leading edge of the plate. An electronic scale was used to measure the mass of frost deposited over the plate. The frost surface temperature was measured by an infrared camera. The combined measurement uncertainties are ±2% and ±5% for the frost layer and density, respectively. More details on the experimental work can be found in Piucco (2008).

Sample plates of a polymeric material (100x100 mm, 2 mm thick) were used during the frost nucleation experiments. Four out of five samples underwent different surface treatments such as the application of car wax and acrylic coating, and surface finishing using rough and fine sand papers. The resulting contact angles were measured

from digital photographs of a water droplet with a known volume on the horizontal surface. The droplet volume was set using a burette with a 0.02 ml scale division. In total, each sample was measured five times at random. An overall uncertainty of ±5° was determined for the contact angle. The surface roughness was measured with a TAYLOR-HOBSON apparatus in a temperature controlled room at 20±1°C. The results obtained for both contact angle and surface roughness are summarized in Tab. 1. The frost nucleation experiments were carried out submitting the five samples to different supercooling degrees, with the conditions of the surroundings held constant at 10°C (temperature), 40% (relative humidity) and 0.7 m/s (air velocity). The supercooling degree was varyied by reducing the chilled plate temperature. The conditions were chosen to keep the dewpoint below 0°C.

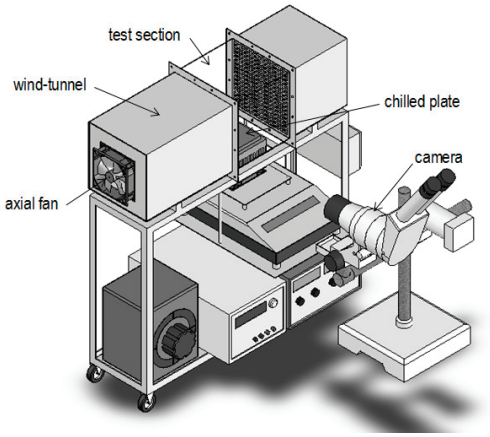

Figure 6. Schematic of the experimental facility

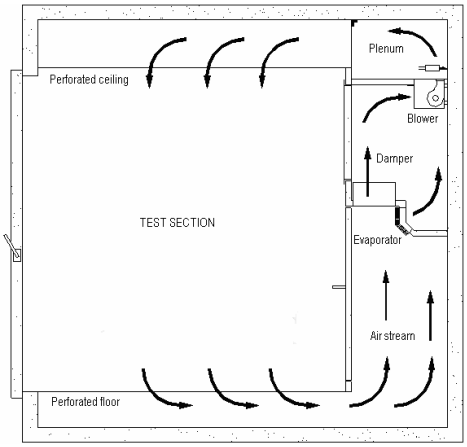

Figure 7. Schematic of the environmental chamber

5. RESULTS AND DISCUSSION

Table 1 summarizes the experimental results in terms of the minimum supercooling degree required to initiate nucleation on each sample. The calculated embryo formation rate, obtained from equation (6), is also reported in Tab.1. It was found that the nucleation limit of the samples whose surfaces underwent a sand paper treatment are lower than that of the original sample (surface I), despite their higher contact angles. This is explained by the higher surface roughness, which favors the occurrence of nucleation. It can also be noted that the supercooling degree of surface III (wax coating) is the highest, which is due to its large contact angle and low roughness. It is believed that the actual roughness of the wax coated sample is lower than the figure in Tab. 1 because of the low mechanical resistance that the wax layer offers against the pressure of the measurement needle. It is also worth noting that the minimum embryo formation rate varied by 40 orders of magnitude.

Table 1. Summary of measured contact angle, surface roughness, and minimum supercooling degree

Sample	θ [degrees]	Roughness [μm]	ΔT_{sup} [°C]	I [embryo/cm^{2}s]
I. Original	72.6	0.05	3.2	$9.6\ 10^{11}$
II. Acrylic coating	83.6	0.11	3.0	$8.4\ 10^{2}$
III. Wax coating	96.7	0.06	4.6	$2.5\ 10^{-11}$
IV. Fine sand paper	118.6	3.37	3.0	$5.4\ 10^{-19}$
V. Rough sand paper	129.5	6.92	2.8	$8.6\ 10^{-30}$

Volmer and Flood (1934) naked-eye observations suggest that a rate of 2.2 embryo/cm²s is required for the onset of nucleation. In this work, the experiment of Volmer and Flood (1934) was reproduced using an aluminum plate with θ=90°, when a minimum nucleation rate of $2.8 \cdot 10^{-4}$ embryo/cm²s was found. This apparent discrepancy can be explained based on the sensitivity of the embryo formation rate with respect to the supercooling degree. As can be seen in Fig. 8, the variation of the embryo formation rate from $2.8 \cdot 10^{-4}$ to 2.2 embryo/cm^{2}s corresponds to a supercooling degree difference of 0.22°C; less than half of the measurement uncertainty (0.5°C). It can also be observed that a variation of ±0.5°C in the supercooling degree produces a variation of 7 orders of magnitude in the embryo nucleation rate. Additionally, if the measurement uncertainty of the contact angle (±5°) is accounted for (Tab. 2), the uncertainty of the embryo formation rate reaches the magnitude of 10^8 embryo/cm²s. Because of this extreme sensitivity, a fixed embryo formation rate of 2.2 embryo/cm^{2}s (Volmer and Flood, 1934) was adopted in this study.

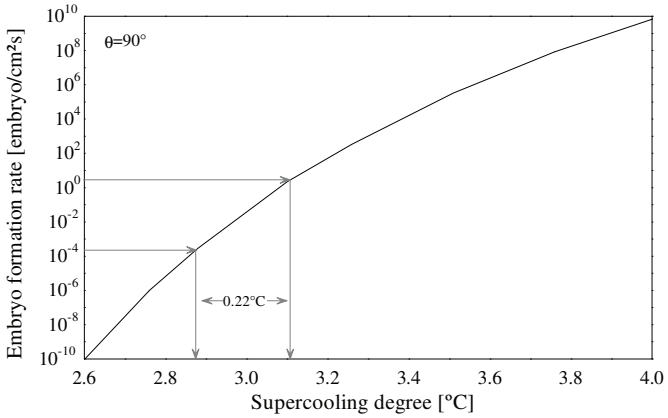

Figure 8. Variation of the embryo formation rate with the supercooling degree (θ=90°)

Table 2. Variation of the embryo formation ratio with the contact angle (ΔT_{sup}=3.1°C)

***θ* [degrees]**	85	90	95
***I* [embryo/cm²s]**	$3.3\ 10^{3}$	$2.0\ 10^{0}$	$1.2\ 10^{-3}$

Figure 9 compares the model predictions with the experimental data summarized in Tab. 1, where a reasonable agreement can be observed. It can be seen that the model slightly underestimates the supercooling degree of the surfaces with lower contact angles (I to III), whereas an opposite behavior is observed for the surfaces with higher contact angles (IV and V). This can be explained by the combined effect of the contact angle and surface roughness, since the latter effect was not accounted for by the theoretical model. Figure 9 also compares the model predictions with experimental data obtained by Na and Webb (2003), showing a good agreement, especially for lower contact angles.

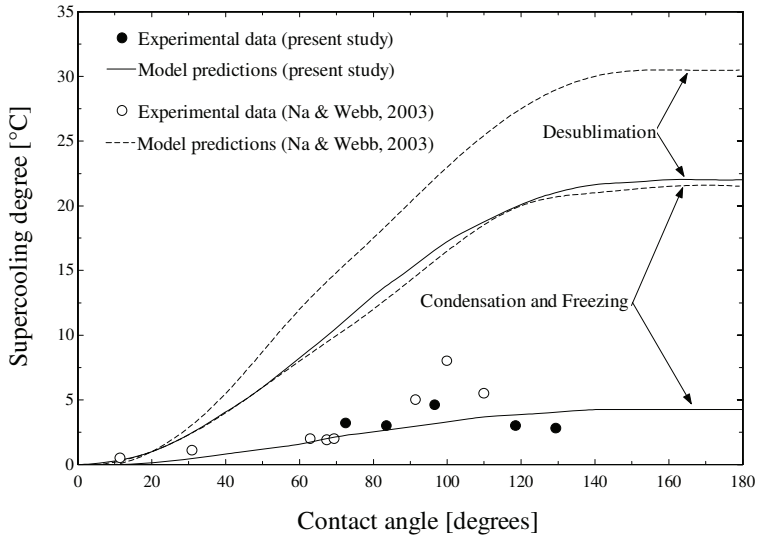

Figure 9. Comparison between experimental data and model predictions

The predictions of the Na and Webb (2003) model are also shown in Fig. 9 (dotted lines). It is clear that their model predictions are not close to the experimental data. This is due to the $\theta=\cos^{-1}(\gamma_{ew}-\gamma_{sw})/\gamma_{se}$ term employed by them instead of $\theta=\cos^{-1}(\gamma_{sw}-\gamma_{ew})/\gamma_{se}$ (Fletcher, 1970), which provided wrong predictions for the nucleation thresholds. Such a mistake induced the authors to the erroneous conclusion that the discrepancies between the model predictions and their own experimental data are due to the fact that the model does not consider the surface roughness. Based on their model predictions, the authors also suggested that efforts had to be made on the development of high contact angle surfaces in order to delay nucleation. However, as shown in Fig. 9, a supercooling degree of 5°C is high enough to guarantee nucleation, independently of the contact angle. Moreover, contact angles higher than 140° have no effect upon the supercooling degree.

6. CONCLUDING REMARKS

An experimental facility was developed and constructed for investigating the frost nucleation, growth and densification processes. It consists of an open-loop wind-tunnel apparatus and an image acquisition system to visualize the frost formation over time. Samples of a polymeric material were submitted to different surface treatments in order to vary the contact angle over a broad range. These samples were tested under a fixed environmental condition, changing the surface temperature, and so the supercooing degree, until the nucleation process started. In addition, the fundamentals of frost formation were investigated and a theoretical model for predicting nucleation as a function of the working conditions and surface characteristics was put forward based on the classical nucleation theory (Fletcher, 1970). The model was compared with the experimental data obtained in this work and elsewhere (Na and Webb, 2003), showing a satisfactory level of agreement. The theoretical analysis shows that as the contact angle increases, a higher supercooling degree is needed for frost nucleation to occur. However, for contact angles higher than 140°, the nucleation limit is practically independent of the contact angle. In addition, it was shown that nucleation is guaranteed when the supercooling degree is higher than 5°C, suggesting that surface coatings have a minor effect upon the frost nucleation for most of refrigeration and air-conditioning applications.

NOMENCLATURE

Roman

A	Area [m^2]
G	Gibbs free energy [J]
h	Embryo height [m]
I	Embryo formation ratio [$1/m^2s$]
I_0	Kinetic constant [$1/m^2s$]
k	Boltzmann constant [J/K]
M	Molar mass of water [kg/mol]
n	Number of molecules [-]
P	Partial pressure of steam [Pa]
r	Embryo radius [m]
R	Ideal gas constant [J/molK]
S	Entropy [J]
T	Temperature [K]
U	Internal energy [J]
V	Volume [m^3]

Greek

γ	Surface energy [J/m^2]
ρ	Density [kg/m^3]
θ	Contact angle [degrees]
ω	Humidity ratio [kg/kg]

Subscripts

e	embryo
se	embryo-surroundings interface
ew	embryo-wall interface
lat	latent
s	surroundings
sat	saturation
sw	surroundings-wall interface
tot	total
w	wall

REFERENCES

Becker, R., Doring, W., 1935, Ann. Phys., Lpz., 24, 719

Fletcher, N.H., 1970, The chemical physics of ice, Cambridge University Press, Cambridge, UK

Lee, H., Shin, J., Ha, S., Choi, B., Lee, J., 2004, Frost formation on a plate with different hidrophilicity, IJHMT, 47, 4881-4893

Liu, Z., Wang, H., Zhang, X., Meng, S., Cheng, S., 2007, Influences of surface hidrophilicity on frost formation on a vertical cold plate under natural convection conditions, Experimental Thermal Fluid Science, 31, 789-794

Liu, Z., Wang, H., Zhang, X., Meng, S., Ma, C., 2005, An experimental study on minimizing frost deposition on a cold surface by use of an anti-frosting paint. Part I. Anti-frosting performance and comparison with uncoated metallic surface, Int. J. Refrigeration, 29, 229-236

Na, B., Webb, R., 2003, A fundamental understanding of factors affecting frost nucleation, IJHMT, 46, 3797-3808

Piucco, R.O., 2008, Theoretical and Experimental Analysis of Frost Formation on the Inner Walls of Refrigerated Cabinets, MSc thesis, Federal University of Santa Catarina, Florianopolis, Brazil (in Portuguese)

Tao, Y.X., Besant, R.W., Mao, Y., 1993, Characteristics of frost growth on a flat plate during the early growth period, ASHRAE Symposia, CH-93-2-2, 746-753

Volmer, M., Flood, H., 1934, Z. Phys. Chem. A, 170, 273

Wu, X., Dai, W., Shan, X., Wang, W., Tang, L., 2007, Visual and theoretical analyses of the early stage of frost formation on cold surfaces, J. Enhanced Heat Transfer, 14(3), 257-268

ACKNOWLEDGEMENTS

The authors duly acknowledge *Whirlpool S.A.*, *CNPq* and *FINEP* for their financial support.